FEATURE ARTICLE

Molecular Reorientation of Liquid Water Studied with Femtosecond Midinfrared Spectroscopy

H. J. Bakker,* Y. L. A. Rezus, and R. L. A. Timmer

FOM Institute AMOLF, Kruislaan 407, 1098 SJ Amsterdam, The Netherlands

Received: February 13, 2008; Revised Manuscript Received: June 18, 2008

The molecular reorientation of liquid water is key to the hydration and stabilization of molecules and ions in aqueous solution. A powerful technique to study this reorientation is to measure the time-dependent anisotropy of the excitation of the O−H/O−D stretch vibration of HDO dissolved in D_2O/H_2O using femtosecond midinfrared laser pulses. In this paper, we present and discuss experiments in which this technique is used to study the correlation between the molecular reorientation of the water molecules and the strength of the hydrogen-bond interactions. On short time scales (<200 fs), it was found that the anisotropy shows a partial decay due to librational motions of the water molecules that keep the hydrogen bond intact. On longer time scale (>200 fs), the anisotropy shows a complete decay with an average time constant of 2.5 ps. From the frequency dependence of the anisotropy dynamics, it follows that a subensemble of the water molecules shows a fast reorientation that is accompanied by a large change of the vibrational frequency. This finding agrees with the molecular jumping mechanism for the reorientation of liquid water that has recently been proposed by Laage and Hynes.

Introduction

Many of the characteristic properties of liquid water find their origin in the large number of directional hydrogen-bond interactions present in this liquid. In spite of the strength and high concentration of these hydrogen-bond interactions, water molecules turn out to be surprisingly mobile. As a result, liquid water is extremely fast in rearranging its molecules to enable the solvation of reactants and to take up dissipated energy.[1−4] An important aspect of this rearrangement is the molecular reorientation of the water molecules.

The molecular reorientation of liquid water has been studied with several experimental techniques like NMR,[5−7] dielectric relaxation,[8,9] and THz absorption spectroscopy.[10,11] With these techniques consistent results concerning the rate of molecular reorientation in liquid water were obtained. However, an unfortunate characteristic of these techniques is that only the average reorientation can be measured, and it is not possible to probe the orientational dynamics of subensembles of the water molecules.

The molecules in liquid water show a large variation in hydrogen-bond configurations and associated hydrogen-bond lengths and angles.[12−17] As a result, the absorption bands of the O−H/O−D stretch vibrations of water molecules (that absorb at 3/4 μm) are strongly inhomogeneously broadened: water molecules with long and bent hydrogen bonds absorb at higher frequencies than water molecules with short and linear hydrogen bonds. With femtosecond midinfrared spectroscopy it is possible to spectrally select a subensemble of water molecules and to measure its specific dynamics, like for instance the fluctuations of the hydrogen-bond network[18−27] or the molecular reorientation.[28−36]

The measurement of the orientational dynamics of water via the excitation of the O−H/O−D stretch vibrations relies on the fact that the rotation of the molecule changes the direction of the vibrational transition dipole moment. This method does not work if there are other processes contributing to the change of the direction of the transition dipole moment, like intramolecular and/or intermolecular resonant (Förster) energy transfer between the vibrations. As a result, it is unfortunately not possible to measure the orientational dynamics of the molecules in pure liquid H_2O.[3] Consequently, the reported femtosecond midinfrared measurements of the orientational dynamics of water always refer to HDO molecules dissolved in either normal or heavy water.[28−36] In both cases the dynamics of a hydroxyl group (either O−H or O−D) embedded in a network of isotopically distinct hydroxyl groups are studied. Studying the orientational dynamics of the O−H stretch vibration of HDO:D_2O has the advantage that it is easier to resolve dynamical inhomogeneities, as O−H the stretch vibration of HDO:D_2O is more strongly inhomogeneously broadened than the O−D vibration of HDO:H_2O.[22,25] On the other hand, studying the O−D vibration of HDO:H_2O has the advantage that the lifetime of the O−D vibration is more than two times longer than that of the O−H vibration, thereby allowing the measurement of the orientational dynamics of the O−D group over a significantly longer time interval.

In this Feature Article we will review the studies of the orientational dynamics of liquid water with femtosecond midinfrared spectroscopy of HDO:D_2O[28−33] and HDO:H_2O.[34−36] We will describe the experiments, the methods by which information on the orientational dynamics has been extracted from the data,

* To whom correspondence should be addressed.

10.1021/jp8012943 CCC: $40.75
Published on Web 10/28/2008

H. J. Bakker was born on March 2, 1965 in Haarlem, The Netherlands. He did his Ph.D. studies in the group of Prof. dr. Ad Lagendijk, at the FOM Institute for Atomic and Molecular Physics (AMOLF). From 1991 to 1994, he worked as a post-doc in the group of Prof. dr. Heinz Kurz at the Institute of Semiconductor Electronics at the Technical University of Aachen, Germany. In 1995 he became a group leader at AMOLF, heading the group "Ultrafast Spectroscopy". The research work of the group includes the spectroscopic study of the structure and ultrafast dynamics of water interacting with ions and (bio)molecular systems and the study of the mechanism of proton transfer in aqueous media. In 2001 he became a full professor of Physical Chemistry at the University of Amsterdam, The Netherlands. In 2004, he received the Gold Medal of the Royal Netherlands Chemical Society for his work on the ultrafast dynamics of aqueous systems.

Y. L. A. Rezus was born on September 29th 1978 in Geneva, Switzerland. He studied chemistry and natural sciences at Radboud University Nijmegen, The Netherlands. After his studies, he spent a year as a guest researcher in Dr. H. Rigneault's group at Institut Fresnel in Marseille. He did his Ph.D. under the supervision of Prof. Dr. H. J. Bakker at the FOM Institute for Atomic and Molecular Physics (AMOLF) in Amsterdam. His research interests include ultrafast spectroscopy, nonlinear optics, and single molecule spectroscopy.

R. L. A. Timmer was born on February 18, 1979 in Westerhaar-Vriezenveensewijk, The Netherlands. He studied Applied Physics at the University of Twente and graduated at the National Institute for High Energy Physics (NIKHEF) under the supervision of Prof. dr. ing. B. van Eijk. He is currently working as a Ph.D. student at the FOM institute for Atomic and Molecular Physics (AMOLF) in the group of Prof. dr. H. J. Bakker on the subject of energy and charge transport in liquid water and ice.

and the interpretation of the data in terms of molecular orientational mobilities. We also compare the experimental findings with the results of molecular dynamics simulations of the reorientation of liquid water.[13–15]

Experimental Section

The orientational dynamics of the O−H/O−D stretch vibrations of HDO dissolved in D_2O/H_2O have been studied with polarization-resolved pump−probe spectroscopy.[28−36] In all experiments, the femtosecond midinfrared pump and probe pulses are generated via a sequence of nonlinear frequency-conversion processes that are pumped by the output of a Ti:sapphire multipass and/or regenerative amplifier (800 nm, 1 kHz, pulse energy ≥1 mJ). The midinfrared pump has a wavelength of ∼3 μm (= ∼3300 cm^{-1}) or ∼4 μm (= ∼2500 cm^{-1}), depending on whether the O−H or O−D stretch vibration is being studied.

Pump and Probe Pulse Generation. In most studies the pump pulses are generated via an optical parametric amplification process in a KTP or $KNbO_3$ crystal that is pumped by a part of the 800 nm pulses of the Ti:sapphire laser. To generate 3 or 4 μm pulses in the parametric amplification, the process has to be seeded by 1100 or 1000 nm light, respectively. This seed has been produced with different methods. In one method, a fraction of the 800 nm light is used to generate a white-light continuum.[31,32] Part of this continuum at 1100/1000 nm is parametrically amplified in a BBO (β-bariumborate) crystal. This process is pumped by a pulse at 400 nm that is generated via second harmonic generation of part of the 800 nm pulse,[31] or by part of the fundamental 800 nm pulse.[32] The resulting light pulses at 1100/1000 nm are sufficiently strong to seed the parametric amplification process in KTP[31] or $KNbO_3$.[32] An alternative method to generate the seed pulses is by parametric generation or white-light generation followed by parametric amplification in BBO to generate pulses with wavelengths of 1300−1400 nm (signal) and 2000−2200 nm (idler).[29,30,35,33] Subsequently, the idler pulses are frequency doubled to pulses with a wavelength of 1000−1100 nm in a second BBO crystal, and these pulses then serve as seed in a parametric amplification process in KTP[29,30,33] or $KNbO_3$.[35] In the experiments of refs 34 and 36, the pump pulses at 4 μm are generated via difference frequency mixing of pulses with wavelengths of ∼1330 and ∼2000 nm in a $AgGaS_2$ crystal. These latter pulses are generated via white-light seeded optical parametric amplification in BBO (Spectraphysics OPA) that is pumped by a fraction of the 800 nm pulses.

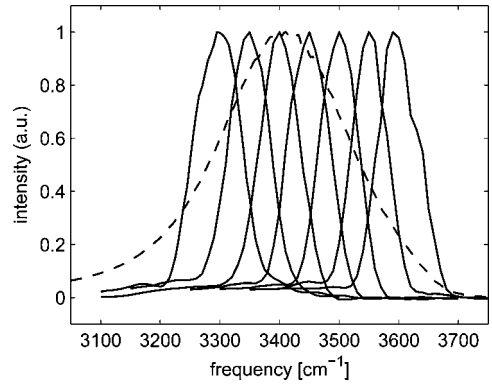

Figure 1. Typical excitation spectra that are resonant with the O−H stretch vibration of a solution of 1% HDO dissolved in D_2O. For comparison also the linear absorption spectrum of the O−H stretch vibration is shown (dashed curve).

The energy of the generated pump pulses varies between 2[34] and 10 μJ.[28−31,33,35] In some studies, the used KTP and $KNbO_3$ crystals are quite short (1 mm) and the 800 nm pulses have a pulse duration of 30[32] or 40 fs.[34,36] The resulting midinfrared pulses are ultrashort, have a pulse duration of ∼50 fs.[32,34,36] The bandwidth of these puleses is ∼400 cm^{-1}, thereby covering completely the O−H/O−D absorption band. In other studies, longer crystals (4−5 mm) and longer 800 nm pulses (∼100 fs) have been used, leading to the generation of longer (∼150 fs) midinfrared pump pulses with a much narrower spectral bandwidth of ∼100 cm^{-1}.[28−31,35] In Figure 1 various pump spectra are presented that are resonant with different parts of the O−H stretch absorption band of HDO:D_2O.

The probe pulses have also been generated with a variety of methods. In some of the experiments,[28,32−35] the probe pulses are obtained by splitting off a small fraction of the pump pulse. In other experiments, independently tunable probe pulses are generated by a separate sequence of nonlinear frequency-conversion processes.[29−31] This sequence can be the same as that used to generate the pump pules.[31] In refs 29 and 30, the probe pulses were generated with the same sequence of frequency conversion processes that was used to generate the pump and probe pulses in ref 34 and 36, i.e., difference frequency mixing in $AgGa_2$ of the signal (1300−1400 nm) and idler (2000−2200 nm) pulses that are generated via white-light seeded optical parametric amplification in BBO.

Vibrational Saturation Spectroscopy. The pump and probe pulses are focused to the same spot in the sample. In the case where the O−H stretch vibration is studied, the solvent is D_2O, and the concentration of HDO is ∼1%. In the case where the O−D stretch vibration is studied, the solvent is H_2O, and the concentration of HDO is somewhat higher, ranging from 2.5−4%. In the latter experiments, a higher concentration has to be used, because the H_2O solvent has a non-negligible absorption in the frequency region of the O−D stretch vibration. Nevertheless, the concentration of O−D oscillators is still sufficiently low to avoid effects of resonant vibrational Förster energy transfer among the O−D vibrations. The samples are either contained in a sample cell with CaF_2 windows [28−31,33−36] or flowed as a 50 μm path length jet.[32] The pump excites a few

percent of the O−D/O−H stretch vibration of the HDO molecule from the $v = 0$ ground state to the $v = 1$ excited state. This excitation leads to a bleaching effect at the fundamental transition frequencies due to a decrease of the $v = 0 \rightarrow 1$ absorption and the presence of $v = 1 \rightarrow 0$ stimulated emission. The excitation also leads to induced absorption at frequencies corresponding to the $v = 1 \rightarrow 2$ transition. The latter absorption is red-shifted with respect to the fundamental transition by 270/200 cm^{-1} due to the anharmonicity of the O−H/O−D stretch vibration. In some experiments, the transmitted probe light is measured spectrally integrated by a PbSe[28−31] or an InSb[32] detector, and in others the transmitted probe is dispersed with a monochromator and detected spectrally resolved by the 32 elements of a MCT (mercury−cadmium-telluride) detector array.[33−36] In all experiments, a small fraction of the probe is split off and used as a reference to correct for the shot-to-shot probe pulse energy fluctuations. In most experiments this reference is measured spectrally integrated,[28,29,31,32,34] but in some experiments the reference is spectrally dispersed in the same way as the probe and detected by another 32 element MCT detector array, thus allowing for a frequency-resolved correction for shot-to-shot fluctuations in the probe−pulse energy.[33,35]

Anisotropy of the Excitation. The rate of molecular reorientation of the water molecules is studied by measuring the time dependence of the anisotropy of the excitation of the O−H/O−D stretch vibration. In most experiments, the polarization of the pump is rotated before the sample at 45° with respect to the probe polarization with a $\lambda/2$ plate. After the sample, the polarization components of the probe parallel and perpendicularly to the pump polarization are alternatingly chosen using a polarizer.[28,29,31−33,35,36] In ref 34, the experiment is performed with a probe pulse that has a polarization that is parallel to the pump polarization, and a probe pulse with a polarization at the magic angle (54.7°) with respect to that of the pump.

The signals measured are the ratios of the transmitted probe and reference beams: $T_{||} = I_{||}/I_{ref}$, $T_{\perp} = I_{\perp}/I_{ref}$, and $T_{iso} = I_{iso}/I_{ref}$, where I_{iso} represents the signal measured by a probe pulse with its polarization at the magic angle. To determine the pump-induced changes $T_{||}$, $T_{\perp}$, and T_{iso}, the signals are alternatingly measured with and without the pump pulse present using a 500 Hz chopper in the pump beam. The signals are used to construct the absorption changes $\Delta\alpha_{||}$, $= \ln[T_{||}/T_0]$, $\Delta\alpha_{\perp} = \ln[T_{\perp}/T_0]$, and $\Delta\alpha_{iso} = \ln[T_{iso}/T_0]$ where T_0 represents the transmission signal in the absence of the pump. From $\Delta\alpha_{||}$ and $\Delta\alpha_{\perp}$, the rotational anisotropy[37] can be constructed

$$R = \frac{\Delta\alpha_{||} - \Delta\alpha_{\perp}}{\Delta\alpha_{||} + 2\Delta\alpha_{\perp}} = \frac{\Delta\alpha_{||} - \Delta\alpha_{\perp}}{3\Delta\alpha_{iso}} \quad (1)$$

The anisotropy can also be obtained from $\Delta\alpha_{||}$ and $\Delta\alpha_{iso}$:[34]

$$R = \frac{\Delta\alpha_{||} - \Delta\alpha_{iso}}{2\Delta\alpha_{iso}} \quad (2)$$

The denominators of eqs 1 and 2 are not affected by the reorientation.[37] Hence, isotropic effects like vibrational relaxation and spectral diffusion are divided out.

Coherent Coupling Effects. When pump and probe pulses overlap, the measured signals will also contrain contributions from coherent coupling effects. One of these effects is resonant four-wave-mixing effect in which the pump and probe set up a $v = 1$ population grating from which the pump is diffracted in the direction of the probe. The influence of this coupling on the anisotropy dynamics is described in detail in ref 31. Another coherent coupling effect is a nonresonant four-wave mixing effect in which the pump and probe create a refractive index grating from which the pump is diffracted in the direction of the probe. Finally, the interaction of pump and probe can lead to a Kerr effect in which the intensity of the pump changes the refractive index experienced over the pulse profile of the probe pulse. This time-dependent refractive index change leads to a spectral shift of the probe that depends on the relative delay of pump and probe.

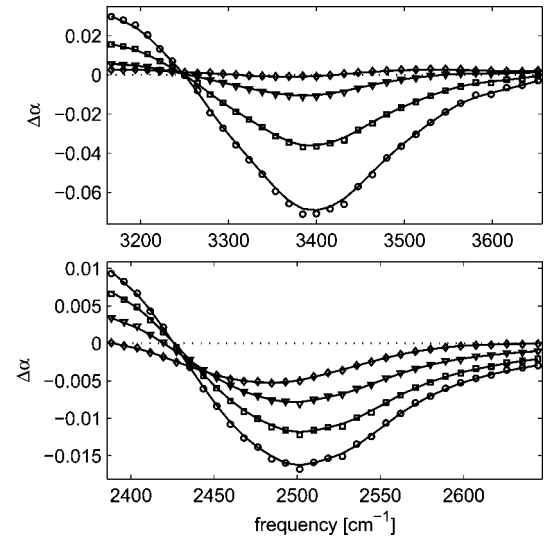

Figure 2. Absorption change as a function of frequency induced by a pump pulse at 3400/2500 cm^{-1} (upper/lower panel) exciting the O−H/O−D stretch vibration of HDO dissolved in D_2O/H_2O. Shown are spectra at delays of 0.5 ps (circles), 1 ps (squares), 2 ps (triangles), and 4 ps (diamonds) between pump and probe. The solid lines represent the results of a fit of the data to the model described in Appendix A.

The coherent coupling effects only occur when pump and probe overlap, i.e., for delays less than or of the order of the pulse duration. In interpreting the data, one should thus be careful in this delay-time regime. The nonresonant four-wave-mixing effect and the Kerr effect can both occur in the water sample and in the windows of a sample cell. Hence, these effects can be diminished by using a free-flowing water jet instead of a sample cell with windows.[32]

Vibrational Relaxation

Experimental Results. In Figure 2, isotropic transient absorption spectra are shown at different delays after exciting the O−H stretch vibration of HDO:D_2O with a pump pulse centered at 3400 cm^{-1} (upper panel) and the O−D stretch vibration of HDO:H_2O with a pump pulse centered at 2500 cm^{-1} (lower panel). At early delays, the transient spectra show the pump-induced bleaching of the fundamental $v = 0 \rightarrow 1$ transition for probe frequencies >3250/2425 cm^{-1} and the induced $v = 1 \rightarrow 2$ absorption at probe frequencies <3250/2425 cm^{-1}. At longer delays (>3 ps) transmission changes are observed that persist over the experimentally accessible time range (500 ps) and that have the character of a bleach on the red side of the spectrum and of an induced absorption on the blue side. These persistent transient spectra reflect the temperature rise in the sample that results from the absorption and thermalization of the energy of the pump pulse. A rise in temperature induces a blue shift and a decrease in cross section of the O−H/O−D vibrations.[33−35]

In Figure 3, the isotropic absorption changes are shown as a function of delay between pump and probe for three different

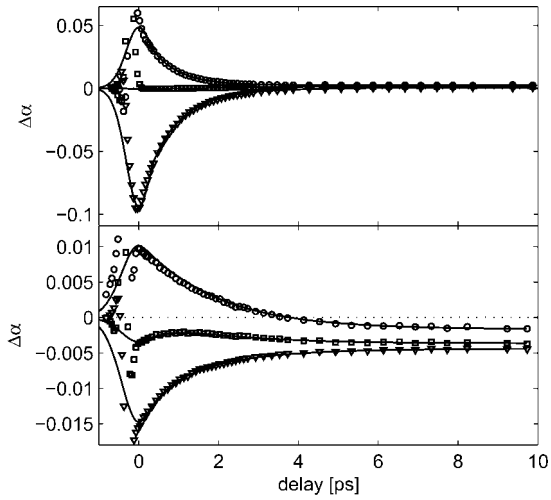

Figure 3. Absorption change as a function of delay between pump and probe for a pump pulse at 3400/2500 cm^{-1} (upper/lower panel) exciting the O−H/O−D stretch vibration of HDO dissolved in D_2O/H_2O. Shown are transients for probe frequencies of 3170/2380 (circles), 3250/2430 (squares), and 3400/2480 cm^{-1} (triangles). The solid lines represent the results of a fit of the data to the model described in Appendix A.

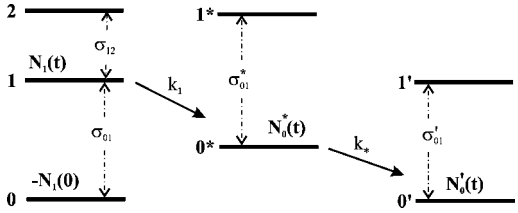

Figure 4. Relaxation scheme of the O−H stretch vibration of HDO dissolved in D_2O and of the O−D vibration of HDO dissolved in H_2O. In the first step of the relaxation the population is transferred from $v = 1$ to an intermediate level $v = 0^*$. In the second step the intermediate level relaxes to the heated ground state $v = 0'$.

probe frequencies. At probe frequencies of 3400/2500 cm^{-1} the signal is dominated by a decaying bleach, whereas at 3170/2390 cm^{-1} the signal consists of a decaying induced absorption. In between these two frequencies more complicated dynamics are observed, especially for the O−D vibration. For a probe frequency of 2435 cm^{-1}, a bleaching signal is observed that shows a decay followed by a rerise to a constant (bleached) end level. The latter ingrowing part of the signal reflects the temperature increase of the sample in the focus of the pump beam. The fact that the signal turns over shows that the temperature rise takes place on a slower time scale than the relaxation of the O−D stretch vibration, which implies that the vibrational relaxation proceeds via a nonthermal intermediate state.

The signal at large delays, which represents the effect of the increase in temperature, is isotropic, meaning that the magnitude of this signal is the same for $\Delta\alpha_{||}$ and $\Delta\alpha_{\perp}$. Hence, to obtain the anisotropy of the excited O−H/O−D vibration, the time-dependent thermalization signal has to be subtracted from $\Delta\alpha_{||}$ and $\Delta\alpha_{\perp}$. To determine the delay dependence of the thermalization signal, the spectral responses of the O−H and the O−D vibration are fitted to a relaxation model that was developed in refs 34, 35, and 38. This model is described in Appendix A and illustrated in Figure 4. In this model the relaxation model proceeds via relaxation with time constant $\tau_1 = 1/k_1$ to an intermediate state. This latter state relaxes with time constant $\tau_* = 1/k_*$ to the final state in which the energy has become

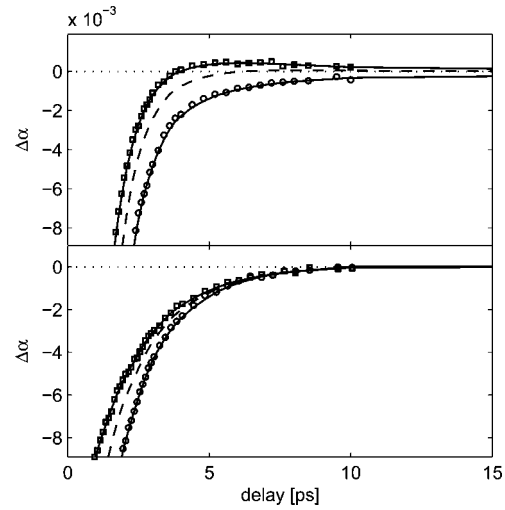

Figure 5. Enlarged parallel (circles) and perpendicular (squares) probing signals measured with a pump pulse at 3400/2500 cm^{-1} (upper/lower panel) exciting the O−H/O−D stretch vibration of HDO dissolved in D_2O/H_2O. The signals are probed at frequencies of 3400/2500 cm^{-1}. The dashed lines represent the isotropic signals $((\Delta\alpha_{||} + 2\Delta\alpha_{\perp})/3)$.

thermal. The two time constants τ_1 and τ_* are treated as global fit parameters, and the cross-sections of the transitions between the vibrational levels are allowed to vary over the spectrum. The resulting fits are represented by the solid lines in Figures 2 and 3. It is seen that the model provides an accurate description of the data, which implies that spectral diffusion effects do not play an important role after a delay of 0.4 ps for pump pulses that are resonant with the center of the absorption bands. For the O−H stretch vibration of HDO dissolved in D_2O $\tau_1 = 0.7 \pm 0.1$ ps and $\tau_* = 0.6 \pm 0.1$ ps. For the O−D stretch vibration of HDO dissolved in H_2O $\tau_1 = 1.8 \pm 0.2$ ps and $\tau_* = 0.9 \pm 0.1$ ps.

In a recent study of the relaxation of the O−H vibration of HDO:D_2O ice, it was also observed that the relaxation proceeds via a nonthermal intermediate state.[39] In this study the intermediate state was observed to relax to a thermalized state with a time constant that depends on the temperature of the ice lattice: at 200 K this time constant is 8.7 ps, and at 270 K this time constant is 5.4 ps.

As the intermediate state is strongly nonthermal in character, it seems likely that the intermediate state is formed by the excitation of an intramolecular vibration of the HDO molecule. With molecular dynamics simulations it was found that the relaxation of the O−H vibration of HDO:D_2O is dominated by energy transfer to the overtone of the bending mode.[40,41] This overtone subsequently rapidly relaxes to the first excited-state of the bending mode. Hence, the intermediate level 0* is likely formed by the first and/or second excited-state of the bending mode of the HDO molecule.

Orientational Dynamics

Extracting the Anisotropy of the Vibrational Excitation. To infer the anisotropy of the excitation from the data, the spectral component corresponding to the heating effect (as obtained from the isotropic spectral dynamics) is subtracted from both $\Delta\alpha_{||}$ and $\Delta\alpha_{\perp}$. Figure 5 shows the resulting $\Delta\alpha_{||}$ and $\Delta\alpha_{\perp}$ for the O−H stretch vibration of HDO:D_2O and the O−D stretch vibration of HDO:H_2O. There is a striking difference between the two vibrations. For the O−D stretch vibration, $\Delta\alpha_{||}$, $\Delta\alpha_{\perp}$, and $\Delta\alpha_{iso}$ decay more or less simultaneously. In contrast, for

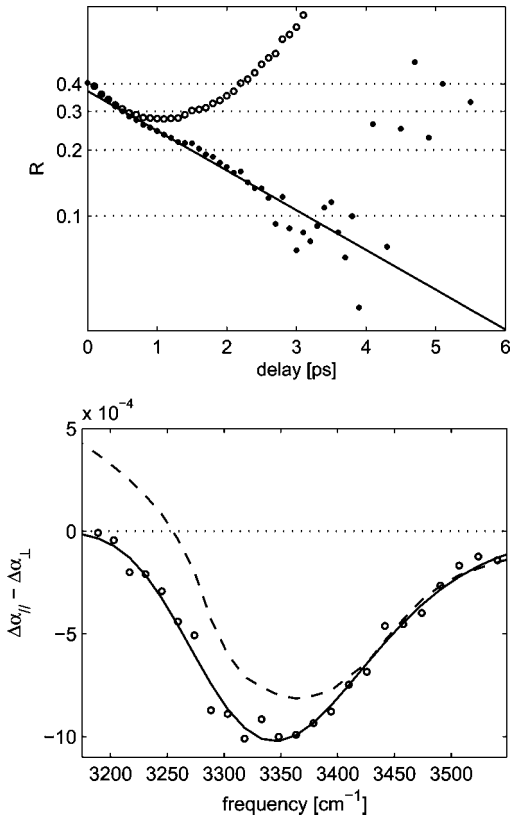

Figure 6. (a) Anisotropy decay as a function of pump−probe delay for the O−H stretch vibration after subtraction of the heating effect (open circles) and after subtraction of the heating effect and correction for the anisotropy of the ground-state that results from the relaxation of the O−H stretch vibration (filled circles). The solid line represents an exponential fit with a time constant of 3 ± 0.2 ps. (b) difference between the parallel and perpendicular probing signals (circles, solid curve) measured for the O−H stretch vibration of HDO in D_2O at a delay of 3 ps. This difference signal represents a bleaching at all frequencies, in contrast to the early time pump−probe signal measured at a delay of 0.3 ps (dashed line).

the O–H stretch vibration, $\Delta\alpha_{||}$ and $\Delta\alpha_{\perp}$ are seen to have non-negligible, opposing amplitudes even after $\Delta\alpha_{iso}$ has vanished. The anisotropy calculated from the curves in the upper panel of Figure 5 is shown in Figure 6a. The obtained anisotropy diverges to infinity, from which it is clear that this curve cannot represent the orientational dynamics of the O−H stretch vibration.

The sign of the residual signals of $\Delta\alpha_{||}$ and $\Delta\alpha_{\perp}$ of the O−H vibration does not depend on whether the original signal is a bleach or an induced absorption.[33] At all frequencies, $\Delta\alpha_{||}$ shows a residual bleaching while $\Delta\alpha_{\perp}$ shows a residual absorption. Figure 6b shows that the amplitude of the residual signal closely follows the linear absorption spectrum of the O−H stretch vibration. The presence of $\Delta\alpha_{||}$ and $\Delta\alpha_{\perp}$ with opposite signs at delays at which there are no excited molecules left ($\Delta\alpha_{iso} = 0$), implies that the vibrational relaxation of the stretch O−H vibration results in a distribution of ground-state molecules that is anisotropic: after relaxation there are more OH groups aligned perpendicular to the pump than there are aligned parallel to it.

The observation of an anisotropic ground-state following vibrational relaxation likely follows from a difference in orientational mobility of excited and nonexcited O−H groups. Directly after the excitation, excited O−H oscillators are oriented preferentially along the pump polarization while the nonexcited O−H oscillators are oriented mainly perpendicular to the pump polarization. In case the excited and the nonexcited oscillators would show the same orientational dynamics, the relaxation of the excited oscillators would restore an isotropic distribution of ground-state O−H oscillators, because the anisotropy of the relaxed oscillators cancels exactly the (opposite) anisotropy of the nonexcited oscillators. However, if the excited oscillators show a faster or slower orientational relaxation at some stage during their relaxation, the distribution of the ground-state O−H oscillators following relaxation will be anisotropic. The eventual depletion of ground-state O−H oscillators that are polarized along the pump polarization indicates that the excited oscillators show a larger orientational mobility at some stage during the relaxation than the nonexcited oscillators. Due to this higher orientational mobility, the relaxed O−H oscillators will be more isotropic than the nonexcited oscillators. The sum of the relaxed oscillators and the nonexcited oscillators will add up to a distribution that is preferentially oriented perpendicular to the pump polarization. As a result, $\Delta\alpha_{||}$ will show a residual bleaching while $\Delta\alpha_{\perp}$ shows a residual absorption, as is observed in the upper panel of Figure 5.

An interesting question is at what stage of the relaxation the excited oscillators show an increased orientational mobility. It is not likely that the oscillators reorient faster while they are in the $v = 1$ state, as it was observed that the $1 \rightarrow 2$ transition shows in fact a slower reorientation than the $0 \rightarrow 1$ transition.[29] Hence, the increased orientational mobility must be present in the intermediate state or in the ground-state directly following the relaxation of the intermediate state. In either case, the increased mobility likely results from a transient high degree of excitation of local librational and hydrogen-bond stretching modes. It has been shown that both scenarios can account for the experimental observations.[33] In case the increased mobility is associated with the intermediate state, a good description is obtained with a time constant $\tau_{or} = 1.7$ ps in the intermediate state $v = 0^*$, and $\tau_{or} = 3.2$ ps in the other states $v = 0$, 1, and $0'$. Alternatively, a good description of the data is obtained by taking the anisotropy to decay by 14% directly following the relaxation to $v = 0'$. In that case τ_{or} is 3 ps for all states.

With molecular dynamics simulations it was shown that the relaxation of the stretch O−H vibration of the HDO molecule proceeds through the overtone of the bending mode.[40,41] The energy gap between the O−H stretch vibration and the overtone of the bending mode is ~500 cm^{-1}, and this energy likely will be released in librational and hydrogen-bond modes. The subsequent relaxation of the intermediate state involves the release of the much larger energy of the overtone of the bending mode of ~2900 cm^{-1}. Hence, the increased mobility of the relaxing molecules most likely occurs after the relaxation of the intermediate state, as this relaxation is expected to result in the highest degree of excitation of intermolecular librational and hydrogen-bond modes.

The measured anisotropy can be corrected for the residual anisotropy of the ground-state by subtraction of this latter contribution. The remaining signal represents the anisotropic signal of the excitation of the O−H stretch vibration only. This anisotropy is represented by the solid curve in Figure 6a. It should be reminded that the O−D vibration does not at all show a residual anisotropy of the ground-state following vibrational relaxation. Possible reasons for this difference are that the vibrational relaxation of the O−D vibration proceeds via a different mechanism and that, as a result of the lower frequency of the vibration, the energy released in the relaxation is not sufficient to induce a significant increase of the orientational mobility of the O−D groups.

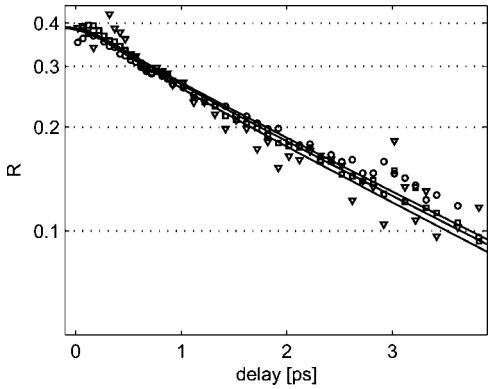

Figure 7. Anisotropy of the O−D stretch vibration of HDO dissolved in H_2O as a function of delay between pump and probe for a pump frequency of 2500 cm^{-1}, and probe frequencies of 2500 (circles), 2550 (squares), and 2600 cm^{-1} (triangles). The points denote the experimental data, the solid lines represent the results of calculations performed with the model described in Appendix B.

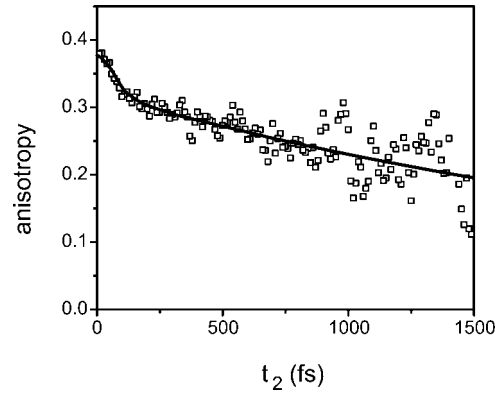

Figure 8. Anisotropy of the O−H stretch vibration of HDO dissolved in D_2O as a function of delay measured with ultrashort (45 fs), broadband (400 cm^{-1}) pump and probe pulses with a central frequency of 3400 cm^{-1} (courtesy of Andrei Tokmakoff). The anisotropy shows a biexponential decay with a fast component in the first 200 fs. Reproduced with permission from *J. Chem. Phys.* **2005**, *122*, 054506.

Average Orientational Dynamics in H_2O and D_2O. Figure 7 shows the anisotropy of the O−D stretch vibration of HDO dissolved in H_2O measured as a function of delay for a pump frequency of 2500 cm^{-1} and three different probe frequencies. The anisotropy signals shown are obtained by correcting the measured $\Delta\alpha_{||}$ and $\Delta\alpha_{\perp}$ for the thermalization signal as determined from the isotropic data. An exponential fit to the data shown in Figure 7 yields a time constant τ_{or} of 2.5 ± 0.2 ps at all probe frequencies, in agreement with earlier results.[35,36,42]

The reorientation time constant of the OD vibration of HDO in H_2O (2.5 ± 0.2 ps) is observed to be somewhat shorter than that of the OH vibration of HDO in D_2O (3 ± 0.3 ps).[29−33] At first sight it may seem surprising that the orientational relaxation of the O−D group proceeds faster than that of the O−H group, as its moment of inertia is almost twice as large. However, there exist two regimes for the reorientation. On very short timescales (<200 fs), the O−H/O−D group can show a limited free rotation (libration) while keeping the donated hydrogen bond intact. This regime will be discussed in the following subsection. On longer timescales, which is of relevance here, the orientational dynamics of the O−H/O−D groups require rearrangements of the water network.[13,14] In this regime the orientational dynamics are no longer determined by the moment of inertia, but instead are governed by the relative motions of the water molecules and, in particular, by the dynamics of hydrogen-bond breaking and reformation. A good measure for the translational mobility of the water molecules is provided by the value of the viscosity. Using the viscosities of H_2O and D_2O (0.9 mPa s and 1.1 mPa s, respectively), the reorientation times of the O−H and O−D are estimated to show a ratio of 0.8, which is very similar to the measured ratio of the reorientation time constants. It should be noted that this finding does not imply that the orientational motion of the water molecules is diffusive. In fact, in a recent molecular dynamics study it was shown that the reorientation involves fast and large angular jumps between different hydrogen-bond configurations.[13] The scaling with the viscosity thus likely follows from the fact that the rate-limiting steps of the reorientation are formed by (translational) molecular motions of which the rate is well characterized by the viscosity.

The measured average molecular reorientation times of 2.5/3 ps in H_2O/D_2O agree well with the results obtained with other techniques. NMR studies also arrive at a reorientation time τ_{or} of the water molecule of 2.5 ps in liquid H_2O.[7] In comparing the results of femtosecond pump−probe and NMR with the results of dielectric relaxation studies and THz absorption, it should be realized that these techniques measure different orientational correlation functions. Femtosecond pump−probe and NMR probe the second order correlation function $\langle P_2 \cos \theta(t)\rangle$, whereas the time constant τ_D that is measured in dielectric relaxation and THz absorption spectroscopy is related to the decay time constant τ_1 of the first order correlation function $\langle P_1 \cos \theta(t)\rangle$. The ratio between the first and second order correlation times τ_1 and τ_2, is determined by the nature of the reorientation mechanism. In the case of pure (small step) rotational diffusion $\tau_1 = 3\tau_2$, but if the reorientation takes places via, for example, jump diffusion, this ratio can be somewhat different.[1]

In dielectric relaxation studies of liquid water, a main relaxation component with a time constant τ_D of 8.3 ps was found.[8] Similar values were found in THz spectroscopic studies of H_2O and D_2O.[9−11] At room temperature the correlation times τ_D of the slow component were determined to be 8.5 ps for H_2O and 10 ps for D_2O. To arrive at the time constant τ_1 of the decay of the correlation function $\langle P_1 \cos \theta(t)\rangle$, the values of τ_D have to be corrected for collective effects. This correction is not without ambiguity, but if we apply the correction proposed by ref 43, we arrive at values of τ_1 of 7.6 and 9 ps for H_2O and D_2O, respectively. When comparing these values with the second order correlation times (2.5 and 3 ps, respectively), one finds a ratio that is close to 3. In addition to the main component with τ_D, dielectric relaxation and THz absorption studies report a weaker and much faster component with a time constant with a value on the order of 100 fs.[9−11] The origin of this fast component will be discussed in the following subsection.

Librational Motions. In Figure 8 the anisotropy of the stretch vibration of HDO:D_2O is shown as a function of delay in the time interval up to 1.5 ps[32] (courtesy of Andrei Tokmakoff). This measurement is performed with midinfrared pulses with a pulse duration of 45 fs. The figure clearly shows that the anisotropy decay takes place on two distinctly different time scales. The anisotropy shows a rapid partial decay in the first 200 fs.[14] Here it should be noted that the signals measured in ref 32 will show little contribution of coherent artifacts because the sample used in this study is a free-flowing water jet. The fast decay is followed by the much slower dominant decay component with a time constant of ∼3 ps.[29−31]

The fast decay time is likely the result of the librational motion of the O−H group, i.e., the hindered rotation of the intact

O−H···O hydrogen-bonded system.[32] This interpretation was recently confirmed by a molecular dynamics study in which it was found that the librational motion indeed leads to a partial decay of the anisotropy in the first 200 fs.[14] The angle of the librational cone can be estimated by assuming that the rotation over this cone leads to the delocalization of an the O−H/O−D dipole over a cone with semiangle θ_0. As was shown by Lipari and Szabo,[44] this leads to a decrease of the initial value of the anisotropy from 0.4 to

$$R(0) = \frac{2}{5}\left[\frac{1}{2}\cos\theta_0(1+\cos\theta_0)\right]^2 \qquad (3)$$

In the experiment shown in Figure 8, the O−H stretch absorption is pumped and probed with broadband infrared pulses. Therefore, the observed librational cone will represent an average over the whole absorption band. In Figure 8, the fast process leads to a decay of the anisotropy to a value of 0.32, which corresponds to a semiangle of free rotation of 22°.

The magnitude of the anisotropy decay due to librations will depend on the frequency of the O−H/O−D vibration. When the frequency increases, the hydrogen bond becomes weaker and the restoring force of the librational motion decreases. As a result, the magnitude of the librational cone will increase. This was indeed observed in a recent study of the initial amplitude of the anisotropy of the O−D vibration of HDO:H_2O. The initial value of the anisotropy was observed to change from 0.36 at 2490 cm^{-1} to 0.32 at 2630 cm^{-1}.[36] Using eq 3, this change in anisotropy value corresponds to a change in librational cone angle from 15° at 2490 cm^{-1} to 22° at 2630 cm^{-1}. For the O–H vibration a similar frequency dependence of the initial amplitude of the anisotropy has been observed.[31] This frequency dependence was explained from the vibration−rotation coupling. If the hydrogen-bond remains intact, this vibration−rotation coupling represents the dependence of the librational motion on the frequency of the O−H frequency. The initial values of the anisotropy observed in ref 31 changes from ∼0.33 at the center of the band at 3410 cm^{-1} to ∼0.27 at 3510 cm^{-1}, which corresponds to an increase of the librational cone angle from ∼20° at 3410 cm^{-1} to ∼28° at 3510 cm^{-1}. The value of ∼20° agrees quite well with the value found in the center of the band found in ref 32 (shown in Figure 8). The frequency dependence of the librational cone has also been calculated with molecular dynamics simulations.[14] It was calculated that at 100 fs after the excitation the librational cone angle is 19° at the center of the band and 25° at a frequency that is 100 cm^{-1} higher. These findings agree well with the experimental observations.[31,32,36]

The amplitude of the librational cones appear to be somewhat larger for the O−H vibration of HDO than for the O−D vibration. For the O−D vibration the librational cone in the center of the band was observed to be 15°,[36] for the O−H vibration it was observed to be ∼22°.[31,32] A likely origin of this difference in amplitude and frequency dependence is the difference in mass of the proton and the deuteron. If the confining potential of the librational motion is harmonic, this difference in mass leads to an amplitude of the librational motion of the O−H group that is $\sqrt{2}$ larger than that of the O−D group.

Frequency Dependence of the Reorientation Dynamics? Femtosecond pump−probe spectroscopy offers the possibility to distinguish the orientational dynamics of water molecules absorbing at different frequencies. In Figure 7, results are presented in which the anisotropy decay is measured at three different probe frequencies in the absorption band of the O−D stretch vibration. At all three probe frequencies, the same single-exponential dynamics are observed, which agrees with the findings of previous studies of the anisotropy dynamics of the O−D stretch vibration of HDO dissolved in H_2O.[34−36] The absence of a frequency dependence of the dynamics of the anisotropy decay suggests that the reorientation is a collective process that is not at all correlated with the strength of the local hydrogen bond.[34]

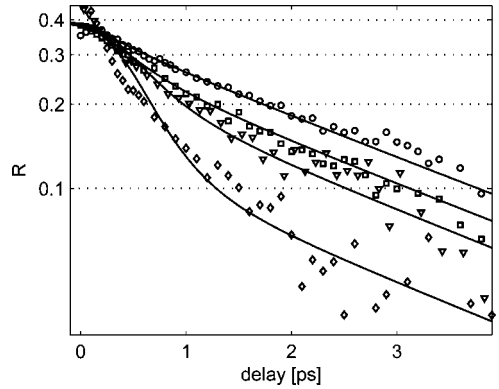

Figure 9. Anisotropy of the O−D stretch vibration of HDO dissolved in H_2O as a function of delay for the same pump and probe frequency of 2500 (circles), 2550 (squares), 2600 (triangles), and 2650 cm^{-1} (diamonds). The points denote the experimental data, the solid lines represent the results of calculations performed with the model described in Appendix B.

Interestingly, in earlier studies of the orientational dynamics of the O−H stretch vibration of HDO dissolved in D_2O, a frequency-dependent anisotropy decay was observed.[28−31] In these studies, the measured anisotropy showed an additional relatively fast component in case the O−H absorption band was excited and probed in the blue wing. It should be noted that this additional faster decay cannot be caused by the presence of a residual anisotropy in the ground-state following the relaxation of the O−H stretch vibration. The effects of this residual anisotropy become apparent only for delays >2 ps, whereas the fast additional decay of the anisotropy is observed for delays <1.5 ps. The additional fast decay can also not be caused by librations. The partial decay of the anisotropy due to librations is nearly complete after 200 fs,[14,32,36] whereas the dynamics observed in the blue wing of the O−H stretch vibration are much slower, having a time constant of ∼700 fs.

It is remarkable that the studies on HDO:H_2O and HDO:D_2O yield such different frequency dependencies. However, it should be realized that these studies also differed in their experimental approach. In the studies of HDO:H_2O the pump was tuned to the center of the absorption band,[34−36] whereas in the studies of HDO:D_2O, the pump was also tuned to other frequency positions.[28−31] The deviation from a single exponential decay was primarily observed when the pump and probe are both resonant with the blue wing of the absorption band.[28−31] Hence, the reported differences in frequency dependence may not be due to the isotopic character of the probed oscillator but rather due to the dependence of the dynamics on the frequency of the excitation. To test this idea, we performed an experiment on the O−D stretch vibration of HDO:H_2O in which the pump pulse is tuned through the absorption band and in which the dynamics are detected at a probe frequency that corresponds to the central frequency of the pump pulse. In Figure 9, the thus measured anisotropy of the O−D stretch vibration is shown as a function of delay for four different pump and probe frequencies. When both pump and probe are tuned to the blue wing, the anisotropy of the O−D vibration shows an accelerated anisotropy decay in the first picosecond after the excitation, in agreement with the earlier observations for the vibration.[28,30,31]

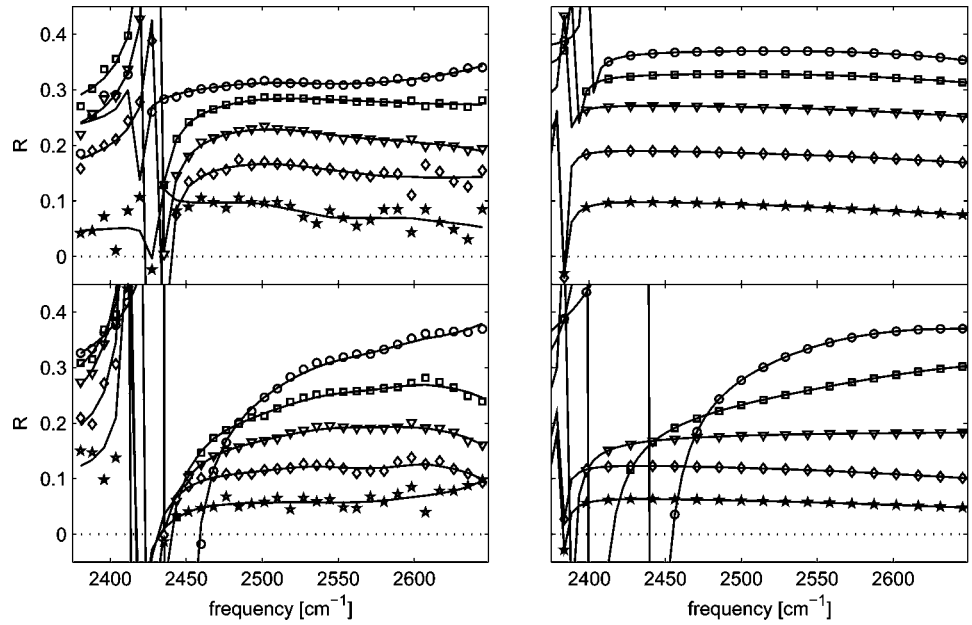

Figure 10. Anisotropy as a function of frequency at delays of 0.2 (circles), 0.5 (squares), 1 (triangles), 2 (diamonds), and 4 ps (stars). shown are results obtained with a pump frequency of 2500 (upper panels) and 2600 cm^{-1} (lower panels). The left panel show the experimental results, the right panels present calculated results obtained with the model described in Appendix B.

Jumping Water Molecules. To study the origin of the accelerated decay of the anisotropy, we probe the spectral dependence of the anisotropy of the O−D stretch vibration of HDO dissolved in H_2O for two different pump frequencies and five different delays. The results are shown in Figure 10. When the O−D stretch vibration is pumped close to its central frequency (upper panels), the anisotropy is nearly the same at all probe frequencies, except in the frequency region where the bleaching changes into an induced absorption. In this frequency region the signal results from the competition of these two signals which leads to an erratic behavior of the anisotropy. With increasing delay, the anisotropy decays show the same decay dynamics at all probe frequencies. This finding agrees with the results shown in Figure 7 and found in refs 34−36.

When the pump frequency is tuned to the blue wing of the absorption spectrum (lower panels of Figure 10), the anisotropy is observed to become strongly frequency dependent in the first few picoseconds. An interesting observation is that the anisotropy in the center and the red wing is significantly lower than 0.4, already at a delay of 0.2 ps. This observation shows that directly after the excitation, the signals in the center and in the red wing contain a significant contribution of water molecules that have reoriented. This fast anisotropy decay cannot be due to librations, because librations lead to a fast partial anisotropy decay[14,32] of which the magnitude decreases with decreasing frequency,[14,36] which is thus opposite to the results shown in Figure 10. In Figure 11, the dynamics of the anisotropy at different probe frequencies are shown following excitation in the blue wing of the absorption band. It is clearly seen that in the center and the red wing the anisotropy starts at a very low initial value, rises and then decays again with the long-time reorientation time constant of ∼2.5 ps.

The low value of the anisotropy in the center and the red wing following excitation in the blue wing (lower panels of Figure 10) cannot be due to a high intrinsic reorientation rate of molecules absorbing in the center and the red wing. The upper panels of Figure 10 clearly show that water molecules absorbing in the center and the red wing in fact show a slow reorientation. Therefore, the large fraction of reoriented molecules in the center

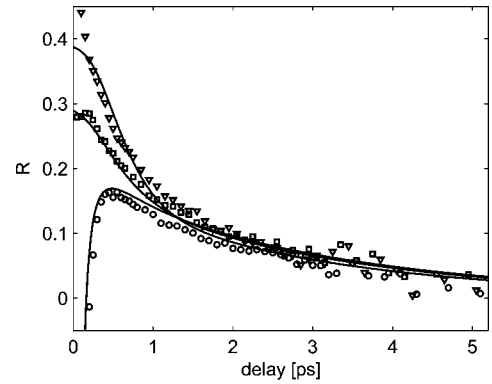

Figure 11. Anisotropy of the O−D stretch vibration of HDO dissolved in H_2O as a function of delay measured for a pump frequency of 2650 cm^{-1} and probe frequencies of 250 (circles), 2550 (squares), and 2600 cm^{-1} (triangles). The points denote the experimental data, the solid lines represent the results of calculations performed with the model described in Appendix B.

and the red wing following excitation in the blue wing must be due to excited molecules that reorient while jumping from the excited blue wing to the center and the red wing of the absorption band. This finding closely agrees with the molecular jump model for reorientation that was developed by Laage and Hynes based on molecular dynamics simulations.[13] In this model, the reorientation involves the breaking of the old hydrogen bond and the formation of a new hydrogen bond, which leads to a large and abrupt change in the frequency of the O−D vibration. In case the pump pulse is tuned to the blue wing of the absorption band, there will be few molecules directly excited in the center and the red wing of the absorption band. As a result, the relative contribution to the signal of molecules that have reoriented and jumped will be relatively large at these frequencies, leading to a low anisotropy already at early delays. A significant part of the frequency jumps takes place within 100 fs, as no initial fast anisotropy decay could be resolved in the center and the red wing of the absorption band. In the blue wing of the absorption band, the number of directly excited molecules is large and the relative contribution of molecules

that have reoriented and have jumped to all possible frequencies in the absorption band will be small. Hence, in the blue wing the initial anisotropy is high.

We compare the data with calculated results obtained with a phenomenological model for the anisotropy dynamics that includes the spectral diffusion of liquid water.[12−17,19−24,27,32] The spectral diffusion of water has been shown to contain both slow and fast components. The slow component of the spectral diffusion has been modeled with a single time constant with a value of ∼1 ps[12−17,19−24,27,32] and with two time constants of ∼0.4 and ∼1.8 ps.[25] Here we describe the slow component of the spectral diffusion as a Gaussian spectral diffusion process (weak frequency modulation limit) with an exponentially decaying frequency correlation function $\langle \delta\nu(t)\delta\nu(0)\rangle = e^{-t/\tau_c}$ with a time constant τ_c of 700 fs. Regarding the fast spectral diffusion two components can be distinguished. The first component is of Gaussian nature (weak modulation limit), and leads to a broadening that is close to the motional narrowing limit. This component is included in the model via the homogeneous line width. We use a value of 80 cm^{-1} for this line width.[21] The other fast component is a spectral diffusion process in which the frequency jumps are of large amplitude leading to a complete loss of correlation to the frequency before the jump (strong frequency modulation limit = nongaussian). This component is only observed for molecules absorbing in the blue wing of the spectrum.[26,27] The jump in frequency has been assigned to the return of a hydroxyl group in a non-hydrogen-bonded configuration to a hydrogen-bonded configuration.[27] The non-hydrogen-bonded configuration is likely a species in which the water molecule forms a weak bifurcated hydrogen bond to two water molecules. The formation of this bifurcated configuration is a concerted process, i.e. involves the gradual approach of a new hydrogen-bonded partner and the simultaneous weakening and bending of the hydrogen bond to the original hydrogen-bonded partner.[27] The return from the bifurcated state to a single strong hydrogen bond can be due to the reformation of the original hydrogen bond or due to the formation of a hydrogen bond to the new partner, i.e., a switching event.[13,27]

In case the evolution through the bifurcated state leads to the formation of a new hydrogen bond, the hydroxyl group has reoriented. Laage and Hynes show that in this case the O−H group has rotated over ∼60°.[13] This angle is quite close to the magic angle of 54.7°. Therefore, in the model, we assume that the switching to a new hydrogen-bonded partner leads to a complete decay of the anisotropy. It is further assumed that switching occurs in 50% of the frequency jumping events. The frequency dependence of the fast spectral diffusion component is described with a phenomenological expression that is fitted to the experimental results of Figures 7, 9, 10, and 11. This expression is given in Appendix B. The rate constant is zero for water molecules with strong hydrogen bonds absorbing in the red wing of the spectrum, and attains a maximum value of 0.5×10^{13} s^{-1} for molecules with very weak hydrogen bonds. In view of the 50% probability that the jump results in reorientation, this rate constant corresponds to a time constant of 100 fs for the frequency jumping in the isotropic data, which is in excellent agreement with the results observed for the frequency jumping of ref 27. It should be noted that the zero jumping rate of molecules absorbing in the red wing does not mean that the hydrogen bond of these molecules do not break. These molecules break their hydrogen bonds on a time scale of ∼1 ps because these molecules spectrally diffuse to the blue via the slow Gaussian spectral diffusion process with a time constant of 700 fs. The calculated results are shown in the right-hand panels of Figure 10 and are represented by the solid curves in Figures 7, 9, and 11. It is seen that the model reproduces all experimentally observed trends. The model reproduces the spectral diffusion dynamics shown in Figure 10 and the frequency and delay time dependence of the anisotropy at different excitation frequencies shown in Figures 7, 9, and 11.

Discussion

In Figure 7 and refs 33−35, it is observed that the anisotropy decay does not depend on frequency when the absorption band is pumped at its central frequency. This can now be explained as follows. In the case where the absorption band is pumped in the center, there will be little direct excitation of rapidly reorienting/spectrally jumping molecules. As a result, the anisotropy will be close to 0.4 (librations not considered) and will be the same for all frequencies. The slow spectral diffusion will lead to an ongoing production of blue-shifted molecules. The reorientation and subsequent frequency jumping of these molecules through the absorption band lead to the same decay of the anisotropy at all frequencies with a time constant of 2.5 ps.

For the O−H stretch vibration of HDO dissolved in D_2O, it was observed that the anisotropy shows an accelerated decay in the first picosecond after the excitation when water molecules are pumped and probed in the blue wing of the absorption band. This fast accelerated decay was assigned to a faster intrinsic reorientation of the water molecules in the blue wing.[29,28,30,31] However, this explanation could only be valid if the water molecules would remain in the blue wing after the reorientation. However, reorientation (other than librational motion) involves the breaking of the hydrogen bond and the formation of a new hydrogen bond.[13,14] Hence, the reorientation leads to a complete loss of the memory of the frequency of the O−H/O−D vibration before the reorientation. This loss of memory implies that the reoriented molecules return to all possible frequency positions in the absorption band. The relative contribution of these returning reoriented molecules increases with increasing detuning from the blue pumping frequency. Hence, at early delay times, the anisotropy shows a strong decrease with frequency following blue excitation (lower panel of Figure 10). This frequency dependence vanishes at later delay times because of the spectral diffusion process. This spectral equilibration leads to an accelerated decay of the anisotropy in the blue wing in the first picosecond after the excitation, and a rise of the anisotropy in the red wing (Figure 11). The accelerated decay in the first picosecond observed for blue pumping and probing is thus not the result of a fast accumulation of reoriented molecules at these particular frequency positions but rather due to spectral equilibration. This also explains why the time constant of ∼700 fs of the accelerated decay[28−30] is similar to that of the slow component of the spectral diffusion.[19,20,22,25,32]

The experimental observations shown in Figures 7, 9, and 11 are largely consistent with the recently reported molecular jumping mechanism for reorientation of liquid water by Laage and Hynes.[13,14] However, there is also a difference between the experimental results and this theory. According to the theoretical work, the probability of a water molecule to evolve to the bifurcated transition state for reorientation should not be dependent on frequency.[14] This prediction is not confirmed by the experimental observations that show a clear dependence of the anisotropy dynamics on the excitation frequency (Figures 10 and 11). The theoretical prediction also does not agree with the observation in 2D-IR studies that excitation in the blue wing

leads to a rapid frequency jumping, while excitation in the center and the red wing does not lead to such an effect.[26,27] The experimental results thus indicate that the molecular dynamics simulations of refs 1 and 2 underestimate the correlation between the frequency of the O−H/O−D oscillator and the jumping probability. This discrepancy could be due to the fact that the classical molecular dynamics simulations of refs 1 and 2 are based on a relatively simple description of the interaction of the water molecules. We hope that the experimental results will stimulate further theoretical work in which the relation between the hydrogen-bond configuration and the probability and mechanism of molecular reorientation is investigated.

The large jumping probability in the blue wing of the spectrum is probably not the result of a direct excitation of molecules in the bifurcated transition state, as this state is extremely short-lived.[13,14,27] Therefore, the transition state configuration itself will contribute negligibly to the absorption, even in the blue wing of the absorption band. In light of the above, the frequency dependence of the jumping probability has to result from the fact that molecules absorbing in the blue wing have a higher probability to evolve to the transition state: for water molecules with long and/or bent hydrogen bonds, the approach of a second hydrogen-bond partner will be easier and more frequent than for water molecules with short and straight hydrogen bonds.

Conclusions

We present and discuss the work on the molecular reorientation of liquid water performed with polarization-resolved femtosecond midinfrared spectroscopy. In these experiments, the reorientation dynamics is probed by measuring the anisotropy dynamics of the excitation of the O−H or O−D stretch vibration of isotopically diluted water. An advantage of femtosecond midinfrared spectroscopy over other techniques is that the tuning of the excitation and probing frequency the technique allows for the distinct measurement of the dynamics of different subensembles of water molecules.

At short delay times after the excitation (<200 fs), the anisotropy was found to show a partial decay due to the librational motions of the water molecules.[31,32,36] These librations have a limited amplitude (cone angle) that depends on the strength of the hydrogen-bond interaction. As a result, the partial decrease of the anisotropy increases from ∼15% at the center of the absorption to ∼30% in the blue wing of the absorption band. At the same hydrogen-bond strength, the librational cone angle is somewhat larger for O−H[31,32] than for O−D,[36] which can be well explained from the difference in mass of H and D.

At intermediate delay times between 200 fs and 1 ps, the anisotropy dynamics strongly depend on the frequency of excitation. In case the water molecules are excited in the blue wing of the O−H/O−D vibration, a fraction of the molecules is observed to show a rapid change in frequency that is accompanied by reorientation. This finding agrees with the molecular jump model for reorientation that was recently proposed by Laage and Hynes.[13,14] In this model the reorientation of a water molecule follows from the evolution of the O−H···O hydrogen bond to a double, bifurcated hydrogen-bond with two other water molecules. The breaking of one of these bonds and the contraction of the other leads to a large change in frequency of the O−H/O−D. If the evolution through the bifurcated state leads to the formation of a hydrogen bond with a new partner (switching event), this leads to an effective rotation of the O−H/O−D group over ∼60°.[13] The rapid change in frequency following excitation in the blue wing has also been observed in recent vibrational correlation echo measurements of the spectral dynamics of isotopically diluted water.[26,27]

At longer delay times (>1 ps), the anisotropy shows the same decay with a time constant of 2.5 ps at all excitation and probing frequencies. In the case where the absorption band is pumped in the center, as was the case in the previous studies of the orientational dynamics of the O−D vibration of HDO:H_2O,[34,35] there will be little direct excitation of rapidly reorienting/spectrally jumping molecules. At all frequencies, the observed reorientation results from molecules that slowly diffuse to the blue where they undergo reorientation followed by a frequency jump through the absorption band. This process leads to the same decay of the anisotropy at all frequencies with a time constant of 2.5 ps. In the case of excitation in the blue wing, as was done in previous studies of the vibration of HDO:D_2O vibration, the rapid frequency jumps cause the early time value of the anisotropy to show a strong decrease with decreasing frequency. The subsequent exchange of the anisotropy at different frequencies due to the slow spectral diffusion process (with a time constant of ∼700 fs), leads to a partial decay of the anisotropy in the blue wing with this time constant. After the spectral equilibration is complete, the anisotropy shows again the same decay at all frequencies with a time constant of ∼2.5 ps.

Acknowledgment. The research presented in this paper is part of the research program of the Stichting Fundamenteel Onderzoek der Materie (Foundation for Fundamental Research on Matter) and was made possible by financial support from the Nederlandse Organisatie voor Wetenschappelijk Onderzoek (Netherlands Organization for the Advancement of Research).

Appendix A: Relaxation Model

The delayed thermalization observed in Figure 3 shows that the energy of the excited O−H/O−D vibration is not directly converted into heat but is first transferred to an intermediate level. This relaxation mechanism can be described with the model that is illustrated in Figure 4. The decay of the O−H/O−D stretch vibration is described with the following set of equations:

$$\frac{dN_1}{dt} = -k_1 N_1$$
$$\frac{dN_0^*}{dt} = k_1 N_1 - k_* N_0^*$$
$$\frac{dN_0'}{dt} = k_* N_0^* \qquad (4)$$

where τ_1 is the relaxation time constant of the $v = 1$ state of the O−H/OD vibration and τ_* is the relaxation time constant of the intermediate level. The equations can be integrated to yield the following expressions for the populations:

$$N_1(t)/N_1(0) = e^{-k_1 t}$$
$$N_0^*(t)/N_1(0) = \frac{k_1}{k_* - k_1}(e^{-k_1 t} - e^{-k_* t}1)$$
$$N_0'(t)/N_1(0) = \frac{k_1}{k_* - k_1}e^{-k_* t} - \frac{k_*}{k_* - k_1}e^{-k_1 t} + 1 \qquad (5)$$

The time-dependent absorption change that results from the populations of the different levels is given by

$$\Delta\alpha_{iso}(\omega,t) = N_1(t)\sigma_{12}(\omega) - [N_1(0) + N_1(t)]\sigma_{01}(\omega) + N_0^*(t)\sigma_{01}^*(\omega) + N_0'(t)\sigma_{01}'(\omega)$$
$$= N_1(t)\sigma_{12}(\omega) + [-N_1(0) - N_1(t) + N_0^*(t) + N_0'(t)]\sigma_{01}(\omega) + N_0^*(t)\Delta\sigma_{01}^*(\omega) + N_0'(t)\Delta\sigma_{01}'(\omega) \quad (6)$$

where $\sigma_{01}(\omega)$ is the ground-state spectrum, $\sigma_{01}^*(\omega)$ is the spectrum of the intermediate state, $\sigma_{01}'(\omega)$is the spectrum of the ground-state after thermalization of the pump energy, and $\sigma_{12}(\omega)$ is the excited-state spectrum. The cross-section differences $\Delta\sigma_{01}^*(\omega)$ and $\Delta\sigma_{01}'(\omega)$ are given by $\Delta\sigma_{01}^*(\omega) = \Delta\sigma_{01}^*(\omega) - \sigma_{01}(\omega)$ and $\Delta\sigma_{01}'(\omega) = \Delta\sigma_{01}'(\omega) - \sigma_{01}(\omega)$. The change in cross-section following thermalization is related to the absorption change at large delays $\Delta\alpha_f(\omega)$ by:

$$\Delta\alpha_f(\omega) = N_1(0)\Delta\sigma_{01}'(\omega) \quad (7)$$

Substitution of eq6 in eq 7 yields

$$\Delta\alpha_{iso}(\omega,t) = N_1(t)\sigma_{12}(\omega) + [-N_1(0) - N_1(t) + N_0^*(t) + N_0'(t)]\sigma_{01}(\omega) \quad (8)$$

$$+N_0^*(t)\Delta\sigma_{01}^*(\omega) + \frac{N_0'(t)}{N_1(0)}\Delta\alpha_f(\omega) \quad (9)$$

Substituting the expressions for the populations into this equation, we obtain

$$\Delta\alpha_{iso}(\omega,t) = N_1(0)[\sigma_{12}(\omega) - 2\alpha_{01}(\omega)]e^{-k_1 t} + N_1(0)\Delta\sigma_{01}^*(\omega)\frac{k_1}{k_* - k_1}(e^{-k_1 t} - e^{-k_* t}) + \Delta\alpha_f(\omega)\left\{\frac{k_1}{k_* - k_1}e^{-k_* t} - \frac{k_*}{k_* - k_1}e^{-k_1 t} + 1\right\} \quad (10)$$

The first term of the last expression represents the bleaching of the fundamental transition and the absorption of the excited $v = 1$ state. The second term represents the change in absorption associated with the occupation of the intermediate state, and the third term represents the change in absorption resulting from the thermalization.

Appendix B: Kinetic Model for the Jumping Mechanism of the Reorientation of Liquid Water

We describe the jumping mechanism for the reorientation of the O−H/O−D groups with a simple kinetic model. In this model the $v = 0 \rightarrow 1$ and $v = 1 \rightarrow 2$ absorption bands are described with Gaussian spectral profiles. These profiles are given by

$$S_{mn}(v) = e^{4\ln 2(v - v_{c,mn})^2/\Delta_{mn}^2} \quad (11)$$

with $v_{c,mn}$ the central frequency of the transition $v = m \rightarrow n$ and Δ_{mn} the full-width-at-half-maximum of this transition. For the $v = 0 \rightarrow 1$ transition $v_{c,01} = 2500$ cm^{-1} and $\Delta_{01} = 156$ cm^{-1}. For the $v = 1 \rightarrow 2$ transition, we use the same spectral shape but shifted by the anharmonic shift of 150 cm^{-1}. Hence, $v_{c,12} = 2350$ cm^{-1} and $\Delta_{12} = 156$ cm^{-1}.

The spectra are divided into bins that each have a width of 4.855 cm^{-1}. The Gaussian spectral diffusion is described by letting the bins exchange population with their next-nearest neighbors with time constants that are given by

$$k_{d,i\rightarrow i+1} = \begin{cases} k_g S_{mn}(\nu)_{i+1}/S_{mn}(\nu)_i & S_{mn}(\nu)_{i+1} < S_{mn}(\nu)_i \\ k_g & S_{mn}(\nu)_{i+1} > S_{mn}(\nu)_i \end{cases}, \quad (12)$$

For each initial population distribution of the bins, the final spectral distribution of the bins will acquire the shape of the spectral function S_{mn}. The rate constant k_g is related to the time constant τ_c of the frequency correlation function via $1/k_g = \tau_c(1 - \gamma)$.[45] The parameter γ depends on the width of the Gaussian equilibrium distribution: $\gamma^2 = 1 - 4/w^2$, with w the half-width at 1/e of the maximum of the equilibrium distribution. In our calculation we use $\tau_c = 700$ fs, w was equal to 19.5 bins, and thus $\gamma = 0.9947$ and $1/k_g = 3.7$ fs.

The fast frequency jumping is described by including an additional process in which every bin transfers population to all other bins. The rate of this transfer strongly depends on the frequency of the water molecule. We describe this frequency dependence with the following expression:

$$k_{j,mn}(r) = \frac{A}{1 + e^{-b(v - v_{j,mn})}} \quad (13)$$

A fit to the experimental data of Figures 4 and 6 yields $A = 0.5 \times 10^{13}$ s^{-1}, $b = 0.1$, and $v_{j,01} = 2543$ cm^{-1}. It should be noted that these parameters are the only fit parameters, the other parameters like τ_c and the homogeneous line width are obtained from other experimental work. For the $1 \rightarrow 2$ transition, we use the same frequency dependence shifted by the anharmonic shift of 150 cm^{-1}: $v_{j,12} = 2393$ cm^{-1}.

The anisotropy decay is calculated by defining anisotropic and isotropic spectral changes $\Delta\alpha_{mn,ani}(v, t)$ and $\Delta\alpha_{mn,iso}(v, t)$ for both the $v = 0 \rightarrow 1$ and $v = 1 \rightarrow 2$ transitions. The anisotropic population change is defined as the population change probed by a probe pulse with a polarization parallel to that of the pump, minus the population probed with a probe pulse with perpendicular polarization. The excitation by the pump pulse, which is assumed to be a Gaussian with a pulse duration of 0.2 ps, results in spectral holes $\Delta\alpha_{01,ani}(v, t)$ and $\Delta\alpha_{01,iso}(v, t)$ and to induced absorption bands $\Delta\alpha_{12,ani}(v, t)$ and $\Delta\alpha_{12,iso}(r, t)$. The frequency dependence of $\Delta\alpha_{mn,ani}(v, t)$ and $\Delta\alpha_{mn,iso}(v, t)$ follow from the central frequency and the spectral width of the pump pulse, the spectral profiles of the $v = 0 \rightarrow 1$ and $v = 1 \rightarrow 2$ transitions defined by eq 11, and the homogeneous line width. The frequency dependence of the bands $\Delta\alpha_{12,ani}(v, t)$ and $\Delta\alpha_{12,iso}(v, t)$ are assumed to be the same as that of the holes $\Delta\alpha_{01,ani}(v, t)$ and $\Delta\alpha_{01,iso}(v, t)$, but shifted by the anharmonic shift of 150 cm^{-1}. The amplitudes are also taken to be the same. This follows from the fact that $\Delta\alpha_{01,ani}(v, t)$ and $\Delta\alpha_{01,iso}(v, t)$ contain the contributions of both the bleaching of the $v = 0 \rightarrow 1$ transition and the $v = 1 \rightarrow 0$ stimulated emission, while on the other hand the cross-section of the $v = 1 \rightarrow 2$ transition is approximately two times larger than the cross-section of the $v = 0 \rightarrow 1$ (and $v = 1 \rightarrow 0$) transition.

In the slow Gaussian spectral diffusion process both the frequency-integrated isotropic and the anisotropic populations are conserved. In the fast frequency jumping process, only the frequency-integrated isotropic population is conserved, the anisotropic population decays. The jumping rates are taken two times larger for the isotropic population than for the anisotropic population, because the jumping can result both in the formation of a new hydrogen bond (reorientation) and in the reformation of the original hydrogen bond (no reorientation). The population changes at all times are calculated using a fourth-order Runge−Kutta scheme. The isotropic and anisotropic spectral changes are used to construct the frequency- and time-dependent anisotropy $R(v, t)$

$$R(v,t) = \frac{\Delta\alpha_{01,ani}(v,t) - \Delta\alpha_{01,ani}(v,t)}{\Delta\alpha_{01,iso}(v,t) - \Delta\alpha_{01,iso}(v,t)} \quad (14)$$

The model includes the effects of the interference of the bleaching of the $0 \rightarrow 1$ transition with the induced $1 \rightarrow 2$

excited-state absorption. This interference influences the anisotropy in the red wing of the absorption where the $0 \rightarrow 1$ bleaching overlaps with the $1 \rightarrow 2$ induced absorption. We find that the interference especially affects the observed anisotropy if the absorption band is excited in the blue wing. In that case, the bare early time $0 \rightarrow 1$ bleaching shows a strong decrease of the anisotropy with decreasing frequency due to the jumping. The $1 \rightarrow 2$ absorption shows the same frequency dependence as the $0 \rightarrow 1$ bleaching, but shifted to lower frequencies by the anharmonic shift of $\sim$150 cm^{-1}. Hence, in the red wing of the bleaching, the blue wing of the $1 \rightarrow 2$ absorption with a relatively high anisotropy is added to the red wing of the $0 \rightarrow 1$ bleaching that has a relatively low anisotropy. The resulting anisotropy is not the average of these anisotropy values, because the two signals have opposite signs. The addition will lead to a net bleaching signal with an even lower anisotropy than the bare $0 \rightarrow 1$ bleaching. Hence, the addition of the $1 \rightarrow 2$ absorption will further enhance the decrease in anisotropy going down from 2600 cm^{-1}. This behavior is very well reproduced by the model. The model does not include the so-called non-Condon effect, which implies that the absorption cross-section of the O−D stretch vibration depends on the frequency. It has been shown that the cross-section of this vibration increases with increasing hydrogen-bond strength and thus with decreasing transition frequency.[46] The main effect of the non-Condon effect will be that the interference effect of the $0 \rightarrow 1$ and $1 \rightarrow 2$ transitions is somewhat decreased, because the blue wing of the $1 \rightarrow 2$ absorption with a relatively low cross-section is added to the red wing of the $0 \rightarrow 1$ bleaching with a relatively high cross-section.

References and Notes

(1) Woutersen, S.; Bakker, H. J. *Nature* **1999**, *402*, 507.
(2) Lock, A. J.; Bakker, H. J. *J. Chem. Phys.* **2002**, *117*, 1708.
(3) Cowan, M. L.; Bruner, B. D.; Huse, N.; Dwyer, J. R.; Chugh, B.; Nibbering, E. T. J.; Elsaesser, T.; Miller, R. J. D. *Nature* **2005**, *434*, 199.
(4) Deak, J. C.; Pang, Y.; Sechler, T. D.; Wang, Z.; Dlott, D. D. *Science* **2004**, *306*, 473.
(5) Smith, D. W. G.; Powles, J. G. *Mol. Phys.* **1966**, *10*, 451.
(6) Godralla, B. C.; Zeidler, M. D. *Mol. Phys.* **1986**, *59*, 817.
(7) Hardy, E. H.; Zygar, A.; Zeidler, M. D.; Holz, M.; Sacher, F. D. *J. Chem. Phys.* **2001**, *114*, 3174.
(8) Barthel, J.; Bachhuber, K.; Buchner, R.; Hetzenauer, H. *Chem. Phys. Lett.* **1990**, *165*, 369.
(9) Kindt, J. T.; Schmuttenmaer, C. A. *J. Phys. Chem.* **1996**, *100*, 10373.
(10) Rønne, C.; Thrane, L.; Åstrand, P.-O.; Wallqvist, A.; Mikkelsen, K. V.; Keiding, S. R. *J. Chem. Phys.* **1997**, *107*, 5319.
(11) Rønne, C.; Åstrand, P.-O.; Keiding, S. R. *Phys. Rev. Lett.* **1999**, *82*, 2888.
(12) Rey, R.; Moller, K. B.; Hynes, J. T. *J. Phys. Chem. A* **2002**, *106*, 11993.
(13) Laage, D.; Hynes, J. T. *Science* **2006**, *311*, 832.
(14) Laage, D.; Hynes, J. T. *Chem. Phys. Lett.* **2006**, *433* (2006), 80.
(15) Lawrence, C. P.; Skinner, J. L. *J. Chem. Phys.* **2003**, *118*, 264.
(16) Corcelli, S. A.; Lawrence, C. P.; Skinner, J. L. *J. Chem. Phys.* **2004**, *120*, 8107.
(17) Auer, B.; Kumar, R.; Schmidt, J. R.; Skinner, J. L. *Proc. Natl. Acad. Sci. U.S.A.* **2007**, *104*, 14215.
(18) Laenen, R.; Rauscher, C.; Laubereau, A. *Phys. Rev. Lett.* **1998**, *80*, 2622.
(19) Gale, G. M.; Gallot, G.; Hache, F.; Lascoux, N.; Bratos, S.; Leicknam, J.-C. *Phys. Rev. Lett.* **1999**, *82*, 1086.
(20) Woutersen, S.; Bakker, H. J. *Phys. Rev. Lett.* **1999**, *83*, 2077.
(21) Stenger, J.; Madsen, D.; Hamm, P.; Nibbering, E. T. J.; Elsaesser, T. *Phys. Rev. Lett.* **2001**, *87*, 027401.
(22) Stenger, J.; Madsen, D.; Hamm, P.; Nibbering, E. T. J.; Elsaesser, T. *J. Phys. Chem. A* **2002**, *106*, 2341.
(23) Yeremenko, S.; Pshenichnikov, M. S.; Wiersma, D. A. *Chem. Phys. Lett.* **2003**, *369*, 107.
(24) Fecko, C. J.; Eaves, J. D.; Loparo, J. J.; Tokmakoff, A.; Geissler, P. L. *Science* **2003**, *301*, 1698.
(25) Asbury, J. B.; Steinel, T.; Stromberg, C.; Corcelli, S. A.; Lawrence, C. P.; Skinner, J. L.; Fayer, M. D. *J. Phys. Chem. A* **2004**, *108*, 1107.
(26) Steinel, T.; Asbury, J. B.; Corcelli, S. A.; Lawrence, C. P.; Skinner, J. L.; Fayer, M. D. *Chem. Phys. Lett.* **2004**, *386*, 295.
(27) Loparo, J. J.; Roberts, S. T.; Tokmakoff, A. *J. Chem. Phys.* **2006**, *125*, 194522.
(28) Woutersen, S.; Emmerichs, U.; Bakker, H. J. *Science* **1997**, *278*, 658.
(29) Nienhuys, H.-K.; van Santen, R. A.; Bakker, H. J. *J. Chem. Phys.* **2000**, *112*, 8487.
(30) Bakker, H. J.; Woutersen, S.; Nienhuys, H.-K. *Chem. Phys.* **2000**, *258*, 233.
(31) Gallot, G.; Bratos, S.; Pommeret, S.; Lascoux, N.; Leicknam, J.-C.; Kozinski, M.; Amir, W.; Gale, G. M. *J. Chem. Phys.* **2002**, *117*, 11301.
(32) Fecko, C. J.; Loparo, J. J.; Roberts, S. T.; Tokmakoff, A. *J. Chem. Phys.* **2005**, *122*, 054506.
(33) Rezus, Y. L. A.; Bakker, H. J. *J. Chem. Phys.* **2006**, *125*, 144512.
(34) Steinel, T.; Asbury, J. B.; Zheng, J.; Fayer, M. D. *J. Phys. Chem. A* **2004**, *108*, 10957.
(35) Rezus, Y. L. A.; Bakker, H. J. *J. Chem. Phys.* **2005**, *123*, 114502.
(36) Moilanen, D. E.; Fenn, E. E.; Lin, Y.-S.; Skinner, J. L.; Bagchi, B.; Fayer, M. D. *Proc. Natl. Acad. Sci. U.S.A.* **2008**, *105*, 5295.
(37) Graener, H.; Seifert, G.; Laubereau, A. *Chem. Phys. Lett.* **1990**, *172*, 435.
(38) Timmer, R. L. A.; Bakker, H. J. *J. Chem. Phys.* **2007**, *126*, 154507.
(39) Iglev, H.; Schmeisser, M.; Simenonidis, K.; Thaller, A.; Laubereau, A. *Nature* **2006**, *439*, 183.
(40) Rey, R.; Hynes, J. T. *J. Chem. Phys.* **1996**, *104*, 2356.
(41) Lawrence, C. P.; Skinner, J. L. *J. Chem. Phys.* **2003**, *119*, 1623.
(42) Piletic, I. R.; Moilanen, D. E.; Spry, D. B.; Levinger, N. E.; Fayer, M. D. *J. Phys. Chem.* **2006**, *110*, 4985.
(43) Wallqvist, A.; Berne, B. J. *J. Phys. Chem.* **1993**, *97*, 13841.
(44) Lipari, G.; Szabo, A. *Biophys. J.* **1980**, *30*, 489.
(45) Burshtein, A. I.; Malinovsky, V. S. *J. Opt. Soc. Am. B* **1991**, *8*, 1098.
(46) Schmidt, J. R.; Corcelli, S. A.; Skinner, J. L. *J. Chem. Phys.* **2005**, *123*, 044513.

JP8012943